

# Dynamic Microgrids in Resilient Distribution Systems with Reconfigurable Cyber-Physical Networks

Yuhua Du, *Student Member, IEEE*, Xiaonan Lu, *Member, IEEE*, Jianhui Wang, *Senior Member, IEEE*, Bo Chen, *Member, IEEE* Hao Tu, *Student Member, IEEE* Srdjan Lukic, *Senior Member, IEEE*

**Abstract**—Modern distribution systems energized by inverter-interfaced distributed generators (DGs) operate as coupled cyber-physical networks (C/P-networks), where the controllable components in the physical network (P-network) are coordinated through the cyber network (C-network). The concept of dynamic microgrids (MGs) operation has been adopted to enable distribution system autonomous operation with varying electric boundaries. To further enhance system operation resiliency and flexibility, dynamic MGs operation with reconfigurable C/P-networks is discussed in this work. An evaluation framework is proposed to assess the operational feasibility of distribution feeders with multiple inverter-based dynamic MGs and come out with possible restoration solutions in the context of cross-layer C/P-network reconfiguration. Furthermore, distributed controllers are developed for components with different operating characteristics to realize seamless system topology variations and provide coordinated secondary regulation in various operation modes. The proposed evaluation framework along with the developed distributed controller has been validated using a Hardware-in-the-Loop (HIL) real-time CPS testbed.

**Index Terms**—Cyber-physical system, distributed control, dynamic microgrids, network reconfiguration

## I. INTRODUCTION

**D**URING extreme events where no substation is available, the islanded distribution system could remain energized by inverter-interfaced distributed generators (DGs) and form inverter-based microgrids (MGs). An islanded inverter-based MG can be treated as a cyber-physical system (CPS) [1]: Dispatchable resources (e.g., energy storage system) with power electronic interfaces are the primary sources that energize the physical network (P-network), while the coordination among multiple inverters is implemented through the cyber network (C-network). To avoid system single point of failure,

distributed control has been favored where each controllable node operates independently and utilizes peer-to-peer communication. Compared to the centralized approach, distributed control features improved resiliency [2].

Conventional MG operates with pre-defined electric boundaries [3]. The distribution feeders could be sectionalized into multiple MGs, each of which interacts at a common point of coupling (PCC). Dynamic MGs as an advanced multi-MG structure has been recently discussed [4], [5]. Compared to conventional MGs with static electric boundaries, dynamic MGs operate with varying structures and interact at dynamic points of interconnection (POI) [6]. The electric topology of a dynamic MG can vary as per the system operator's requests using conventional breakers or advanced switches with remote controllability (e.g. smart switch [SSW] [7]).

Consensus-based algorithms have been frequently utilized in the distributed control of a CPS. Different control objectives for islanded MG operation (e.g., proportional DG output power sharing [8], MG voltage unbalance mitigation [9], average DG operation voltage regulation [10], etc.) can be achieved using consensus algorithms in different forms (e.g., average consensus [11], dynamic consensus [12], etc.). Most existing distributed control algorithms consider static cyber-physical networks (C/P-networks), i.e., both the electric structure and communication topology among controllable nodes are invariant during CPS operation [8]–[10]. Distributed controllers that ensure convergence under C-network with switching topology have been discussed [13], [14]. Due to the nature of consensus algorithm, proper operation of consensus-based control requires that the C-network of controllable DGs remains a connected graph [11], i.e., there exists a path in the C-network that can connect any two nodes. It is noteworthy that though distributed control algorithms that rely on unidirectional communication have recently been discussed, C-networks in the present distribution systems are mainly bidirectional [15].

In conjunction with variations on C-network, the P-network of a CPS should also be reconfigurable so that additional system operation solutions could be enabled [16]. The operation of a CPS with varying P-network could be done in the context of dynamic MGs. Compared to conventional power system topology variation, additional control efforts are needed for inverter-based MGs [17]: Without proper regulation, undesired transients could be generated during the network reconfiguration and damage the power electronic devices, which could potentially de-stabilize the system. A distributed secondary

Manuscript received November 15, 2019; revised February 9, 2020; accepted March 08, 2020. This work was supported in part by the U.S. Department of Energy's Office of Energy Efficiency and Renewable Energy (EERE) under Solar Energy Technologies Office (SETO) Agreement Number 34230. (Corresponding author: Xiaonan Lu)

Yuhua Du and Xiaonan Lu are with the College of Engineering, Temple University, Philadelphia, PA 19122, USA (email: yuhua.du@temple.edu; xiaonan.lu@temple.edu)

Jianhui Wang is with the Department of Electrical Engineering at Southern Methodist University, Dallas, TX, 75275 USA (email: jianhui@smu.edu).

Bo Chen is with the Energy Systems Division, Argonne National Laboratory, Argonne, IL 60439 USA (e-mail: bo.chen@anl.gov).

Hao Tu and Srdjan Lukic is with the Department of Electrical and Computer Engineering at North Carolina State University, Raleigh, NC, 27695 USA (email: ht@ncsu.edu; smlukic@ncsu.edu).

control strategy for dynamic MGs operation and seamless physical reconfiguration have been proposed in [6]. Operation states measured at the target SSW are shared with corresponding inverter-interfaced grid forming DGs for regulation. However, the developed algorithms are only applicable to static C-networks with explicit communication topology.

To fully exploit the operation flexibility of distribution systems with inverter-based dynamic MGs, both its C- and P-networks should be reconfigurable as per the system operator's requests without violating system operation constraints. The independency and interdependency between C- and P-network on the operation of dynamic MGs have been discussed in some works [18], [19]. Both C- and P-network of a CPS could be described by interconnected graphs with nodes and branches. However, their operation mechanisms are inherently different and the topologies of both networks are not necessarily identical. The topology variation of a P-network under normal conditions could only be done through circuit breakers (e.g., SSW). Meanwhile, there are various existing forms of C-networks and their topology variations are only constrained by the availability of the C-network components (e.g., network switches, Ethernet cables, etc.). The interdependency between C- and P-network could be described by the fact that the resilient operation of P-network depends on the functional C-network [18]. P-network reconfiguration with dynamic MGs requires coordinated operation among inverter-interfaced DGs and SSWs, which relies on information exchange through a connected C-network [6]. On the other hand, topology variation on C-network should guarantee the resilient operation of P-network by remaining sufficient connectivity [20]. A general impact assessment approach of unexpected C-network failure on the P-network operation was conducted in [18]. In [19], an analytical method is proposed to quantify the impacts of C-network on MG operation reliability. However, such assessing approach is only applicable for C-networks under a centralized structure. Moreover, it represents passive evaluation over CPS operation, while solutions for active C/P-networks reconfiguration has not been extensively discussed.

In this work, inverter-based distribution system operation in the context of dynamic MGs and reconfigurable C/P-networks are discussed. The main contribution and notable features of this work are listed as follows:

- 1) An evaluation framework is proposed for autonomous distribution systems resilient operation as coupled C/P-networks. The network topology is tracked using a developed disjoint-set data structure with reduced complexity. A set of algorithms are developed to systematically assess the operational feasibility of a CPS under given network topologies. For systems that are not able to operate properly as requested, restoration solutions in the context of active C/P-networks reconfiguration are provided. Two types of network reconfigurations are discussed, namely *physical driven cyber* (P2C) variation and *cyber driven physical* (C2P) variation.
- 2) Detailed controller designs that utilize consensus-based distributed control are developed to implement dynamic MG operation under both P2C and C2P variations, both of which cannot be handled using conventional distributed

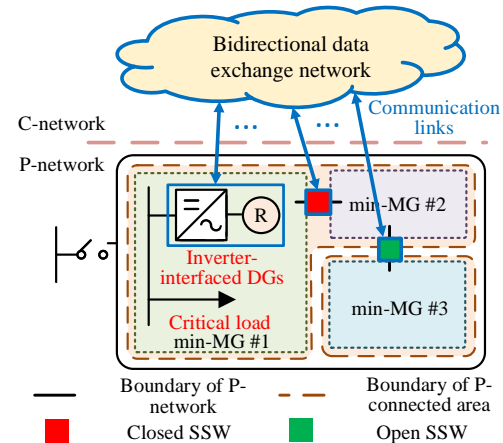


Fig. 1: Dynamic MGs operation structure with reconfigurable C/P-networks

secondary controllers. Besides constant system frequency and voltage regulation, the developed controllers achieve proportional power sharing among connected DGs and seamless system network reconfiguration as requested. Compared to the controllers proposed in [6], the developed controller does not require static C-networks with explicit topology and thus significantly extends system operation flexibility and resiliency. The dynamic performance of the proposed controllers is validated using a Hardware-in-the-Loop (HIL) real-time CPS testbed.

## II. MODELING OF CPS WITH RECONFIGURABLE C/P-NETWORKS

### A. C/P-Networks Structure of Dynamic MGs

In this work, controllable components that interconnected in the C/P-networks are managed as independent agents. Inverter-interfaced DGs with grid-forming capability is selected as the primary resources that energize the distribution system. SSWs are implemented as the circuit breakers that actualize the P-network variation as per the system operator's requests. The system structure under study is presented in Fig. 1.

The system's P-network is implemented in the context of dynamic MGs [5]. As shown in Fig. 1, the whole P-network is sectionalized by SSWs into several min-MGs. Min-MGs is the basic building block that constructs dynamic MGs and is defined as the smallest set of DGs and SSWs that is able to support local critical loads by forming a MG. The electric boundaries of min-MGs are determined by the locations of the SSWs they contain. Each min-MG shall have at least one POI to the rest of the grid via SSW, and two adjacent min-MGs share only one SSW. Neighboring min-MGs that share the same SSW could be interconnected by closed SSWs and operate as a whole, while those who are physically isolated operate independently. The system P-network topology is determined by the connectivity among neighboring min-MGs, which are decided by the on-off status of the corresponding SSWs. P-network variation starts with the reconfiguration request sent by the system operator to the target SSWs that need to change status. Once the seamless transit criterion is met, the target SSW shall change status and the P-network reconfiguration is fulfilled. It is noteworthy that dynamic MGs have shifting electric boundaries, which

is in contrast to conventional multi-MG structure where each individual MG has static topology and interacts with others through static PCCs. Additionally, DGs are managed under static groups in conventional multi-MG structure, which is insufficient for dynamic MGs operation as the DGs should be dynamically re-grouped in response to the system real-time operating topology. Advantages of adopting dynamic MGs over the conventional multi-MG structure has been extensively discussed in existing literature [4], [5], [16].

The C-network describes the system communication topology. As shown in Fig. 1, each agent could exchange selected information with its neighboring agents using bidirectional communication. The connectivity among neighboring agents (either DG agent or SSW agent) in the P-network is limited by the geometric structure of the electric system and the status of SSWs, e.g., DGs can only be physically connected through transmission lines and closed SSWs. However, such limitation does not exist in the C-network, agents that are physically isolated could still be cyber connected and exchange information as requested. At last, the C-network topology under study is non-static. The communication links among agents could be actively reconstructed by the system operator or disabled due to unplanned C-network failure. The availability of each agent is also varying, i.e., agents could cease communication as requested or due to element failure [19].

### B. Graph Theory and Disjoint-set Data Structure

A network is modeled by a graph  $G = (\mathcal{V}, \mathcal{E})$ , with  $\mathcal{V} = \{v_i\}$  being the set of nodes (agents) and  $\mathcal{E} = (v_i, v_j)$  being the set of edges (links). A subgraph  $S$  of graph  $G$  is a graph whose node sets  $\mathcal{V}(S)$  and edge sets  $\mathcal{E}(S)$  are all subsets of  $G$ . In this work, the reconfigurable C- and P-networks could be divided into several connected subgraphs  $(S_1, S_2, \dots, S_m)$  that are respectively isolated. The agents are defined as *connected* if they are subset of the same  $\mathcal{V}(S_i)$ .

Adjacent matrix has been frequently used to describe the topology of a network, where each off-diagonal index indicates the connectivity between two nodes. In this work, the network topology in CPS is described using *Network Matrix*,  $N = A + S$  where  $A = \{a_{ij}\}$  is the adjacency matrix and  $S = \text{diag}(s_i)$  is the operation status matrix. Each DG agent and SSW agent represents a node in the network matrix. The network matrices for both C-network and P-network are modeled respectively:

- To describe a C-network as  $N_C$ ,  $a_{ij} = 1$  if agent  $i$  and  $j$  have peer-to-peer communication links, otherwise  $a_{ij} = 0$ . For both SSW agent and DG agent,  $s_i = 1$  if agent  $i$  is cyber available, otherwise  $s_i = 0$ . In this work, it is defined that  $s_i = 0$  for an open SSW.
- To describe a P-network as  $N_P$ ,  $a_{ij} = 1$  if agent  $i$  and  $j$  belong to the same min-MG, otherwise  $a_{ij} = 0$ . If agent  $i$  is a SSW agent, then  $s_i = 1$  if it is closed and  $s_i = 0$  if open. For DG,  $s_i = 1$  if it is on-line and  $s_i = 0$  if off-line.

As reviewed, the C-network under study are bidirectional, while the P-network are also bidirectional by nature. Thus, the adjacent matrix  $A$  of C/P-networks have mutual interactions between nodes, as  $N(i, j) = N(j, i)$ .

The developed network matrix contains sufficient information regarding the network topology in terms of connected

subgraphs. However, it takes  $\mathcal{O}(n^2)$  storage and searching complexity for a network with  $n$  nodes (agents). In this work, such information is tracked using a disjoint-set data structure which reduces the required storage space and searching complexity to  $\mathcal{O}(n)$  [21]. For a given network with  $n$  agents, each agent is assigned with an ID for presentation purpose and stored in an ID array,  $id()_{1 \times n}$ , where  $id(i)$  represents the assigned ID number for agent  $i$ . Without specification, it is assumed that  $id(i) = i$  by default. A *parent array*,  $par()_{1 \times n}$  and its corresponding *root array*,  $root()_{1 \times n}$  are constructed:

- The parent array is developed from the network matrix to capture the connectivity of each node (agent) with reduced complexity. The  $i$ th index of parent array,  $par(i)$  represents the ID of agent  $i$ 's *parent agent*. Agent  $i$  and its parent agent,  $j = par(i)$  has direct connectivity in the network, as  $n_{ij} = n_{ji} = 1$  which can be directly observed from the network matrix.
- The root array is developed from the parent array to identify the isolated subgraphs each agent belongs to. The  $i$ th index of root array,  $root(i)$  represents the ID of agent  $i$ 's *root agent*, and agents belong to the same connected subgraph if and only if they have the same root agent. Agent  $i$  and its root agent,  $k = root(i)$  is not necessarily directly connected in the network, as  $n_{ik} = n_{ki} \neq 1$  and cannot be directly observed from the network matrix.

Thus, whether two agents are connected in a certain network can be identified by comparing their root agent. The developed root array describes connectivity between two agents with reduced data storage and search complexity. The root array is constructed from the parent array as it can not be directly observed from the network matrix. Agent  $i$  and  $j$  are connected in  $N$  if  $root(i) = root(j)$ . Specific rules that construct the parent array and root array from network matrix are discussed in the following sections.

## III. EVALUATION FRAMEWORK OF A CPS WITH RECONFIGURABLE C/P-NETWORKS

In this section, the operation feasibility criterion of CPS under distributed control is developed. Restoration schemes that search for all the possible C/P-networks reconfiguration options that meet the developed criterion are proposed. It is assumed that the system operator has the knowledge of the operating C/P-networks topology and the ability to request/implement network reconfiguration. The stability criterion of inverter-interfaced DGs operation under the requested physical network should be assessed by the system operator before finalizing the network variation using existing techniques [22]. DG power availability and other system reconfiguration constraints (e.g., renewable/load forecasting, system unbalance mitigation, etc.) are parts of the optimization problem for the system operator to finalize the system optimal operation topology and out-of-the-scope of this work.

### A. Feasibility criterion of CPS with static C/P-Networks

When no reconfiguration is requested, the CPS operates with static C/P-networks and the system is considered as *feasible* if it operates properly. Following theorem regarding system operation feasibility is drawn:

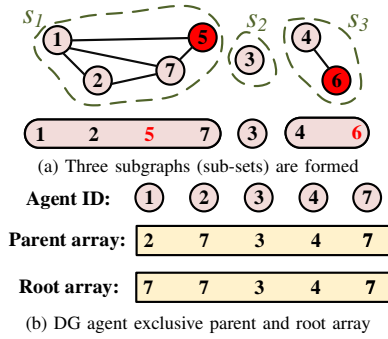


Fig. 2: Sample DG agent exclusive parent and root array constructed for a 7-agent network with 5 DG agents.

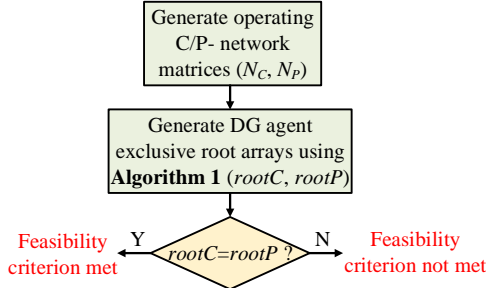


Fig. 3: CPS operational feasibility criterion with static C/P-networks

**Theorem 1** Proper operation of CPS with reconfigurable C/P-networks requires all the DG agents that are physically connected to also be cyber connected, and vice versa.

Detailed proof regarding **Theorem 1** can be found in Appendix A. Referring to the developed disjoint-set data structure, it is concluded from **Theorem 1** that CPS operation feasibility requires the root agent of each DG agent to be identical in both C- and P-networks.

In this work, each DG agent and SSW agent is assigned with an ID. Detailed rules that construct the root array that is DG agents exclusive are developed and can be found in Appendix A as **Algorithm 1**. A sample 7-agent network with 5 DG agents and 2 SSW agents is shown in Fig. 2. For the given network topology, three subgraphs ( $s_1$ ,  $s_2$  and  $s_3$ ) are formed. Agent 1, 2, 3, 4 and 7 are DG agents while agent 5 and 6 are SSW agents, thus the DG agent exclusive ID array is  $id=[1\ 2\ 3\ 4\ 7]$ . The constructed parent array is  $par=[2\ 7\ 3\ 4\ 7]$  and its corresponding root array is  $root=[7\ 7\ 3\ 4\ 7]$ . It is observed from the constructed root array that:

- 1) Three different root agents (7, 3 and 4) are presented, indicating there being three connected subgraphs that are respectively isolated in the network;
- 2)  $root(1) = root(2) = root(5) = 7$ , indicating agent 7 is the root agent of agent 1, 2 and 7 ( $id(1) = 1$ ,  $id(2) = 2$  and  $id(5) = 7$ ) and thus they are connected in the same subgraphs and isolated from the rest agents.

Thus, the network topology in terms of connected subgraphs for DG agents is reduced from a 7-by-7 matrix to a 5-index array. The connectivity among DG agents can be easily checked by comparing their root agent. Once the DG root arrays for C-network,  $rootC()$  and P-network,  $rootP()$  are constructed, **Theorem 1** can be applied to check the feasibility of a CPS with certain C/P-networks: CPS operation feasibility requires the root arrays for both C- and P-network to be

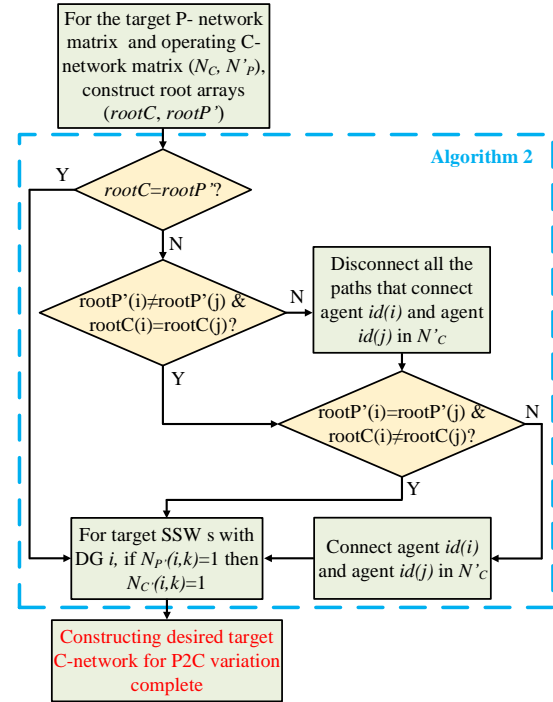


Fig. 4: CPS operation scheme implementing P2C variation identical, i.e.,  $rootC = rootP$ . A flow chart of the developed feasibility criterion is presented in Fig.3.

## B. CPS Restoration Scheme Using P2C Variation

The P-network of a CPS could be actively reconfigured as per the system operator's request. The system P-network topology is determined by the on-off status of SSWs and requires dedicated control efforts to achieve seamless transit. When the system operates under static C/P-networks (operating C/P-networks) and a target P-network topology is requested that requires network reconfiguration, following operation conditions should be met before the target SSW changes status:

- 1) The system operation feasibility criterion should be met once the CPS operates under the target P-network after reconfiguration, i.e., the operating C-network should guarantee feasible CPS operation with the target P-network.
- 2) To guarantee seamless P-network variation, the operation states at the target SSW should be accessible to DGs for regulation during reconfiguration, i.e., the target SSW should not be isolated from DGs in C-network (which is not required in the feasibility criterion).

In case the conditions are not fully met, the CPS can not be properly operated under the target P-network with the operating C-network. To fulfill the requested P-network reconfiguration without violating system operation constraints, the operating C-network could be reconfigured accordingly and such C-network variation is called *P2C variation*.

The P2C variation is developed to implement a C-network reconfiguration before realizing the requested P-network reconfiguration. The desired C-network should meet 1) feasibility criterion with the operating P-network, 2) sufficient connectivity between the target SSW and DGs and 3) feasibility criterion with the target P-network. An operation scheme to implement P2C variation is proposed and presented in

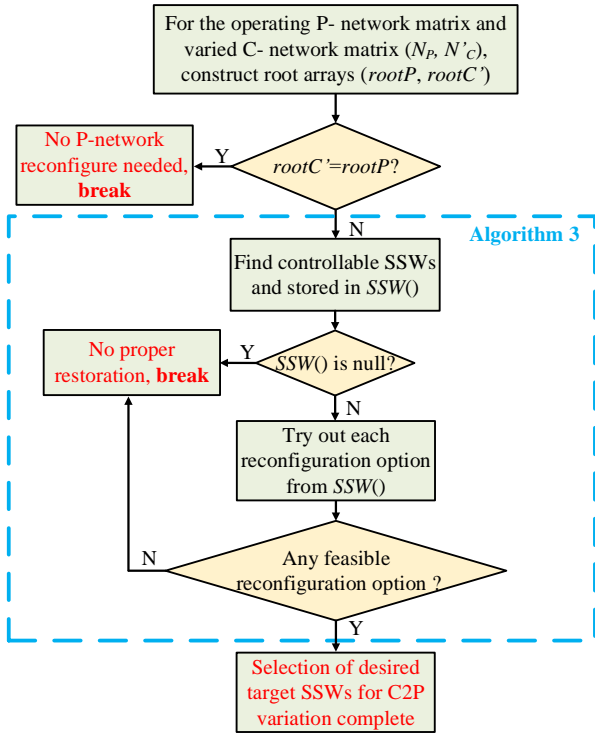


Fig. 5: CPS operation scheme implementing C2P variation

Fig. 4. Detailed rules that construct the desired C-network can be found in Appendix B as **Algorithm 2**. In practice, a successful P-network reconfiguration is determined by the system operator with considerations of many factors. If the operating C-network can not support the requested P-network reconfiguration, the P2C variation could be used to enable more system operation options. By implementing appropriate C-network, CPS operation feasibility criterion is met and the requested P-network variation could be seamlessly executed.

### C. CPS Restoration Using C2P Variation

Similar to P-network, the C-network of a CPS under study is also reconfigurable. When the C-network varies as per the system operator's request, it is assumed that the target C-network has already been well designed to meet the feasibility criterion with the operating P-network. As reviewed, C-network reconfiguration is more flexible compared to the P-network one, and does not require additional control efforts for seamless network transit.

However, if the C-network variation is unplanned, e.g., communication links permanently lost due to element failure during extreme weather, DGs that are physically connected could be isolated in the C-network and the feasibility criterion is not met. To avoid system cascading failure, besides implementing C-network repair, the P-network could also be actively reconfigured to restore the system back to proper operation. Such P-network variation is called *C2P variation*.

The C2P variation is developed to implement a P-network reconfiguration after an unplanned C-network variation that leads to improper CPS operation. To implement a successful C2P variation, the following operation conditions should be met in terms of target SSWs being selected to change status:

- 1) SSWs that are selected as target SSW must be both cyber and physically connected to the same group of DG

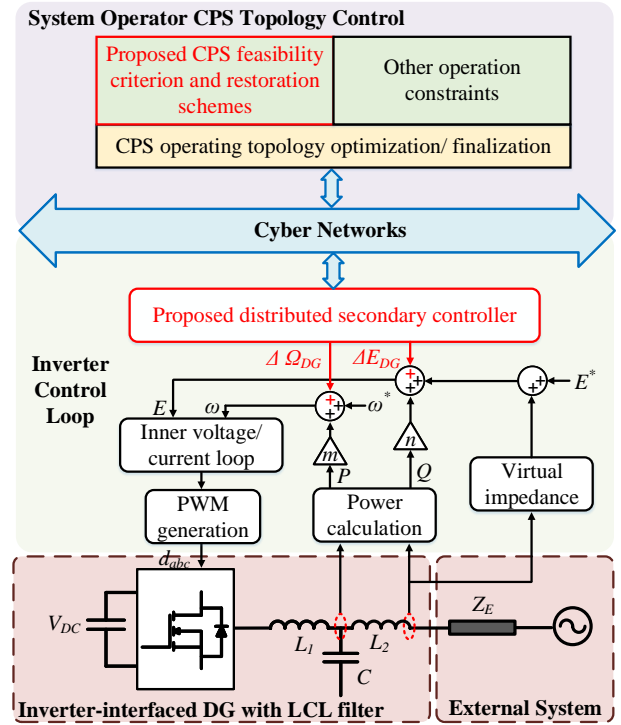


Fig. 6: Proposed control diagram of inverter-interfaced DGs in CPS with reconfigurable C/P-networks

agents. SSWs that are cyber isolated from DGs and are not considered as controllable.

- 2) The system operation feasibility criterion should be met once the CPS operates under the target P-network after reconfiguration. Compared to P2C variation, the operating C-network is not reconfigurable in this case.

An operation scheme to implement C2P variation is proposed and presented in Fig. 5. Detailed rules that construct the desired P-network reconfiguration in terms of target SSWs selection can be found in Appendix B as **Algorithm 3**. In practice, the availability of communication devices can be tracked using heartbeat packets [23] and the system operator should be constantly monitoring the system operation feasibility. Once an unplanned C-network variation is detected that leads to improper CPS operation, the C2P variation could be used for system restoration. By implementing appropriate P-network reconfiguration seamlessly, CPS operation feasibility can be restored with the damaged C-network.

At last, it is noteworthy that compared to individual DG plug-and-play control, the proposed operation schemes utilize reconfigurable C/P-networks in resilient distribution system operation, which require coordinated control among DGs and SSWs and improve CPS operation flexibility.

## IV. DISTRIBUTED CONTROLLER DESIGN FOR DYNAMIC MGS WITH RECONFIGURABLE C/P-NETWORKS

Besides constructing C/P-networks that meet the CPS operation feasibility criterion, proper controller designs for the controllable components in the CPS are also critical to maintaining system proper operation with reconfigurable C/P-networks. The control diagram of inverter-interfaced DG under study is shown in Fig. 6. The proposed CPS feasibility criterion and restoration schemes are implemented by the system operator,



while detailed distributed controllers for SSW agents and DG agents are proposed to fulfill the requested network reconfiguration. Specifically, for inverter-interfaced DGs, hierarchical control structure for voltage-source-inverter in the inductive system is adopted, where system frequency/active power regulation is decoupled from voltage/reactive power regulation [24]. Grid-forming DGs with sufficient power capacity are under study, while grid following renewable resources with intermittent power outputs (e.g., photovoltaic) are treated as part of uncontrollable load variation.

### A. Frequency/Active Power Regulation

The system frequency/active power regulation controllers for DG agent  $i$  are proposed:

$$\omega_i = \omega^* - m_i P_i + \Delta\Omega_{DG,i} \quad (1a)$$

$$\Delta\dot{\Omega}_{DG,i} = -k_f \Delta\omega_i - k_P \Delta P'_{ij} - \Delta\Omega_{SSW,i} \quad (1b)$$

where  $\omega_i$  and  $\omega^*$  are DG operating and rated frequency;  $m_i$  is  $P$ - $f$  droop gain;  $P_i$  is DG active power output;  $\Delta\Omega_{DG,i}$  is the secondary control variable;  $k_-$  represent control gains;  $\Delta\omega_i = \omega_i - \omega^*$  represents DG operating frequency regulation;  $\Delta P'_{ij} = \sum a_{ij}(P'_i - P'_j)$  represents proportional active power sharing among DG agent  $i$ 's cyber connected DG agents, where  $P'_i$  is the per-unit active power of DG agent  $i$ ;  $\Delta\Omega_{SSW,i} = \sum a_{ij}\Delta\Omega_{SSW,j}$  represents accumulated regulation efforts from DG agent  $i$ 's cyber connected SSW agents, where  $\Delta\Omega_{SSW,j}$  is control variable from SSW agent  $j$ .

When the system converges, terms on the right side of (1b) equal to zero, respectively. The first term ensures the system operates under rated frequency, as  $\omega_i = \omega_j = \omega^*$ . The second term achieves proportional active power sharing among DGs that are cyber connected, as  $\Delta P'_{ij} = \sum a_{ij}(P'_i - P'_j) = 0$ . For any DG  $i$ , it is guaranteed by the proposed feasibility criterion that there exists at least one DG  $j$  that satisfies  $a_{ij} = 1$  and thus  $P'_i = P'_j$ . The last term is determined by the SSW controller with respect to the system operator's request.

When the CPS operates under static C/P-networks and the SSW agent receives no network reconfiguration request, the developed control variable from SSW agent  $j$  to agent  $i$  is:

$$\Delta\Omega_{SSW,j} = \frac{k_P}{N_{SSW,j}} (\sum a_{ji} P'_i + \sum a_{jk} \Delta\Omega_{SSW,k}) - \Pi_P \quad (2)$$

where  $N_{SSW,j}$  is the total number of agents that are cyber connected to SSW agent  $j$ ;  $\Pi_P$  is defined as  $\Pi_P = k_P P'_i$  if agent  $i$  is DG agent and  $\Pi_P = 0$  if agent  $i$  is SSW agent. Equation (2) represents proportional active power sharing among DGs that are both physical and cyber connected through closed SSWs.

When SSW agent  $j$  is requested to re-open/re-close, it ceases data exchange with neighboring SSW agents and inputs local measurements accordingly to connected DG agents:

$$\begin{cases} \Delta\Omega_{SSW,j} = k_{\Delta P} \Delta P'_{SSW,j} & \text{to DG, if re-open} \\ \Delta\Omega_{SSW,j} = k_{\Delta\theta} \Delta\theta_{SSW,j} & \text{to DG, if re-close} \\ \Delta\Omega_{SSW,j} = 0 & \text{to SSW} \end{cases} \quad (3)$$

where  $\Delta P'_{SSW,j}$  is the per-unit through active power at SSW agent  $j$  when it is closed and  $\theta_{SSW,j}$  is the voltage phase mismatch at SSW agent  $j$  when it is open. Equation (3) achieves system seamless P-network reconfiguration: As the controller converges, on the target SSW, the through active

power is minimized before it re-opens; and the voltage phases on both sides are synchronized before it re-closes.

### B. Voltage/Reactive Power Regulation

The system voltage/reactive power regulation controllers for DG agent  $i$  are proposed:

$$E_i = E^* - n_i Q_i + \Delta E_{DG,i} \quad (4a)$$

$$\Delta\dot{E}_{DG,i} = -\gamma_i k_E \Delta E_i - k_Q \Delta Q'_{ij} - \Delta E_{SSW,i} \quad (4b)$$

$$V_i = E_i - k_V \int a_{ij}(V_i - V_j) dt \quad (4c)$$

$$\gamma_i = -k_\gamma \int a_{ij}(\gamma_i - \gamma_j) dt \quad (4d)$$

where  $E_i$  and  $E^*$  are DG operating and rated voltage;  $n_i$  is  $Q$ - $V$  droop gain;  $Q_i$  is DG reactive power output;  $\gamma_i$  is the designed control variable that enables/disables DG voltage regulation and  $\gamma_i(0) = 1$ ;  $\Delta E_{DG,i}$  is the secondary control variable;  $\Delta E_i = V_i - E^*$  represents average DG voltage regulation, where  $V_i$  is the observed average DG voltage;  $\Delta Q'_{ij} = \sum a_{ij}(Q'_i - Q'_j)$  represents DG proportional reactive power sharing regulation, where  $Q'_i$  is the per-unit reactive power of DG agent  $i$ ;  $\Delta E_{SSW,j}$  is from SSW agent  $j$ .

When the system converges, terms on the right side of (4b) equal to zero, respectively. The first term ensures the average DG voltage is regulated as rated when  $\gamma_i = 1$  and  $V_i = V_j = E^*$ , while DG agent  $i$  ceases its voltage regulation when  $\gamma_i = 0$ . The second term achieves proportional reactive power sharing among DGs that are directly cyber connected as  $\Delta Q'_{ij} = \sum a_{ij}(Q'_i - Q'_j) = 0$  and thus  $Q'_i = Q'_j$  similar to the active power case. The last term represents regulation as requested by the system operator. Equation (4c) is formed using a standard dynamic consensus algorithm and represents a distributed average DG voltage observer. It is proved in [12] that as the system converges,  $V_i = V_j = \frac{1}{n} \sum E_i$ . Equation (4d) is formed using a standard average consensus algorithm and acts as a distributed signal indicator. It is proved in [11] that as the system converges,  $\gamma_i = \gamma_j$ .

When no network reconfiguration is requested, the developed control variable from SSW agent  $j$  to agent  $i$  is:

$$\Delta E_{SSW,j} = \frac{k_Q}{N_{SSW,j}} (\sum a_{ji} Q'_i + \sum a_{jk} \Delta E_{SSW,k}) - \Pi_Q \quad (5a)$$

$$V_j = \frac{1}{N_{SSW,j}} \sum a_{ji} V_i \quad (5b)$$

$$\gamma_j = -k_\gamma \int a_{ji}(\gamma_j - \gamma_i) dt \quad (5c)$$

where  $Q'_i$  is the per-unit reactive power outputs from DG agent  $i$  and  $\Delta E_{SSW,k}$  is the control variable from SSW agent  $k$ ;  $\Pi_Q = k_Q Q'_i$  if agent  $i$  is DG agent and  $\Pi_P = 0$  if agent  $i$  is SSW agent. For DGs that are both physical and cyber connected through closed SSWs, proportional DG reactive power sharing regulation is enabled in (5a) and average DG voltage regulation in (5b). Equation (5c) represents DG voltage regulation enable/disable control and it is observed that SSW agents with no reconfiguration request do not determine the voltage regulation status of their cyber connected DGs.

When SSW agent  $j$  is requested to re-open/re-close, it ceases data exchange with neighboring SSW agents and inputs local measurements to connected DG agents:

$$\begin{cases} \Delta E_{SSW,j} = k_{\Delta Q} \Delta Q'_{SSW,j} & \text{to DG, if re-open} \\ \Delta E_{SSW,j} = k_{\Delta V} \Delta V_{SSW,j} & \text{to DG, if re-close} \\ \Delta E_{SSW,j} = 0 & \text{to SSW} \end{cases} \quad (6)$$

where  $\Delta Q'_{SSW,j}$  is the per-unit through reactive power at SSW agent  $j$  when it is closed;  $\Delta V_{SSW,j} = V_{SSW,j} - E^*$  where  $V_{SSW,j}$  is the voltage magnitude at SSW agent  $j$  when it is open. As (6) converges on the target SSW, the through reactive power is minimized before it re-opens and the voltage magnitudes on both sides are regulated as rated before re-close.

At last, the enable/disable status of average DG voltage regulation is determined by system control objectives. It has been pointed out in [24] that simultaneous regulations on multiple DG operation voltage and DG proportional reactive power sharing can not always be achieved, and thus when voltage regulation with higher priority is requested (e.g., SSW voltage synchronization in P2C variation) or identical voltage regulation can not be guaranteed (e.g., SSW operation in C2P variation), average DG voltage regulation on corresponding DG agent  $i$  should be disabled. Such distributed indicator is realized using pinning-based consensus [25]:

$$\begin{cases} \gamma_j = 1 & \text{to DG, if re-open in P2C} \\ \gamma_j = 0 & \text{to DG, if in C2P or re-close in P2C} \\ \gamma_j = 0 & \text{to SSW} \end{cases} \quad (7)$$

It is observed from (7) that the target SSW agent  $j$  acts as a pinning input and by setting  $\gamma_j = 0$ , average DG voltage regulations are disabled on connected DG agents, as  $\gamma_i = \gamma_j = 0$  when controller converges. Once the network variation is done and no upcoming reconfiguration is requested, average DG voltage regulation could be brought back by re-setting  $\gamma_i = 1$  on each DG agent  $i$ .

### C. Convergence and Stability Analysis

Following lemmas are used for subsequent stability analysis:

**Lemma 1** [26]: If  $\mathbf{M}$  is positive-definite and  $\mathbf{N}$  is a positive-definite scalar, then  $\mathbf{MN} = \mathbf{NM}$  is positive-definite and  $\mathbf{M} + \mathbf{N}$  is positive-definite.

**Lemma 2** [27]: Characteristics polynomial in the following forms:  $\det(s^2\mathbf{I} + s\mathbf{A}_1 + \mathbf{A}_2) = 0$  has all its roots satisfy  $\text{Re}(s) < 0$  if both  $\mathbf{A}_1$  and  $\mathbf{A}_2$  are positive-definite.

**Lemma 3** [6]:  $\mathbf{M} = \text{diag}(M_i)$  is positive-definite scalar and  $\mathbf{L}$  is a Laplacian Matrix of a connected graph.  $\mathbf{L} + r[\mathbf{1}]_n\mathbf{M}$  is positive-definite when  $r$  is a positive constant.

It is assumed that the inverters are stable under primary control and the CPS operation feasibility criterion is met. The dynamics of inverter inner current/voltage loop are assumed to be fast enough and can be ignored. For inverters that are physically connected, system operating status are modeled [6]:

$$\dot{\delta}_i = -m_i \frac{E' E^*}{X_i} \delta_i + \Delta \Omega_{DG} \quad (8a)$$

$$\omega_v^{-1} \dot{E}_i = -E_i - n_i \frac{E^*}{X_i} \cos \delta' E_i + \Delta E_{DG} \quad (8b)$$

where the delay in adjusting DG output frequency is ignored, while the delay in adjusting DG output voltage magnitude

is modeled as a first-order low-pass filter [27].  $X_i$  is the equivalent reactance between the  $i$ th inverter and PCC. Denote  $M_i = \frac{E' E^*}{X_i}$  and  $N_i = \frac{E^*}{X_i} \cos \delta'$  as constants. At last, denote  $\mathbf{M} = \text{diag}(M_i)$ ,  $\mathbf{N} = \text{diag}(N_i)$ ,  $\mathbf{m} = \text{diag}(m_i)$  and  $\mathbf{n} = \text{diag}(n_i)$ . Denote  $[\mathbf{1}]_{\mathbf{M},\mathbf{N}}$  as a  $\mathbf{M}$ -by- $\mathbf{N}$  all ones matrix.

System small signal stability with the proposed frequency/active power regulations is first derived. The linearized system modeling are presented in matrix form as:

$$\dot{\mathbf{X}}_\delta = \mathbf{W}_\delta \mathbf{X}_\delta \quad (9)$$

where  $\mathbf{X}_\delta = (\delta, \Delta \Omega_{DG})$  is system states and  $\mathbf{W}_\delta$  is the corresponding system matrix.

When no reconfiguration is requested, the system matrix is derived as:  $\mathbf{W}_\delta = \begin{pmatrix} -\mathbf{mM} & \mathbf{I} \\ k_f \mathbf{mM} - k_p \mathbf{H}' \mathbf{M} & -k_f \mathbf{I} \end{pmatrix}$ , where  $\mathbf{H}' = \mathbf{L}' + \mathbf{L}'_1$ . Matrix  $\mathbf{L}'$  is the Laplacian matrix that describes direct communication links among DGs from (1b). Two DGs are not necessarily cyber connected and  $\mathbf{L}'$  could contain all zero rows/columns i.e.,  $\mathbf{L}'(k, k) = 0$  where the  $k$ th DG has no direct communication with the other DGs. Matrix  $\mathbf{L}'_1$  describes indirect communication between DGs through SSWs from (2). Each DG is guaranteed to be cyber connected to at least one DG or SSW to maintain a connected cyber network, i.e., it is guaranteed that  $\mathbf{L}'_1(k, k) \geq 1$ . Matrix  $\mathbf{H}'$  is a positive-definite matrix. The characteristic polynomial of  $\mathbf{W}_\delta$  is simplified using Schur complement:  $\det(s\mathbf{I} - \mathbf{W}_\delta) = \det(s\mathbf{I} + k_f \mathbf{I}) \det[s^2\mathbf{I} + s(\mathbf{mM}) + k_p \mathbf{H}' \mathbf{M}] = 0$ . It is observed that  $\det(s\mathbf{I} + k_f \mathbf{I}) = 0$  satisfied  $\text{Re}(s) < 0$  for all its roots. Referring to **Lemma 1**, when  $M_i \approx M_j$ , matrix  $\mathbf{H}' \mathbf{M}$  is positive-definite. Then referring to **Lemma 2**, it is concluded that all the roots of  $\det[s^2\mathbf{I} + s(\mathbf{mM}) + k_p \mathbf{H}' \mathbf{M}] = 0$  satisfy  $\text{Re}(s) < 0$ . Thus under this scenario, the system is exponentially stable if  $M_i \approx M_j$ .

When the target SSW is requested to open, the system matrix becomes:  $\mathbf{W}_\delta = \begin{pmatrix} -\mathbf{mM} & \mathbf{I} \\ k_f \mathbf{mM} - k_p \mathbf{H}_O \mathbf{M} & -k_f \mathbf{I} \end{pmatrix}$

where  $\mathbf{H}_O = \mathbf{H}' + \frac{k_{\Delta P}}{k_P} \mathbf{D}'_O$ . Assume there are  $n_L$  and  $n_R$  DGs on each side of the target SSW. Referring to C2P variation, it is guaranteed  $\mathbf{H}' = \text{diag}(\mathbf{H}'_{n_L, n_L}, \mathbf{H}'_{n_R, n_R})$ . Matrix  $\mathbf{D}'_O$  describes the target SSW through power from (3). Referring to the autonomous system power balance between generation and consumption, it is derived that  $|\Delta P_{SSW}| = |2 \sum_{i \in N_L} P_i - P_L| = |2 \sum_{j \in N_R} P_j - P_L|$  where  $P_L$  is the system total power consumption. It is derived that  $\mathbf{D}'_O = 2 \text{diag}([\mathbf{1}]_{n_L, n_L}, [\mathbf{1}]_{n_R, n_R})$ . Referring to **Lemma 3**,  $\mathbf{H}_O$  is positive-definite. Similar to the previous case, the system is exponentially stable if  $M_i \approx M_j$ .

When the target SSW is requested to close, the system matrix becomes:  $\mathbf{W}_\delta = \begin{pmatrix} -\mathbf{mM} & \mathbf{I} \\ k_f \mathbf{mM} - k_p \mathbf{H}_C \mathbf{M} & -k_f \mathbf{I} \end{pmatrix}$  where

$\mathbf{H}_C = \mathbf{H}' + \frac{k_{\Delta \theta}}{k_P} \mathbf{D}'_C \mathbf{M}^{-1}$ . Matrix  $\mathbf{D}'_C$  describes target SSW phase mismatch from (3). Referring to Millman's theorem [28], voltage phasor measured by SSW could be expressed in a complex form:  $|V_{SSW}|(1 + j\theta_{SSW}) = \sum c_i E_i(1 + j\delta_i)$  where  $c_i = \frac{X_p}{X_i}$  and  $(X_p)^{-1} = \sum (X_i)^{-1}$ . It is derived that  $\mathbf{D}'_C = [\mathbf{1}]_{n, n} \mathbf{D}$  with  $\mathbf{D} = \text{diag}(\frac{E'}{|V_X|} c_i)$ . When  $M_i \approx M_j$ ,

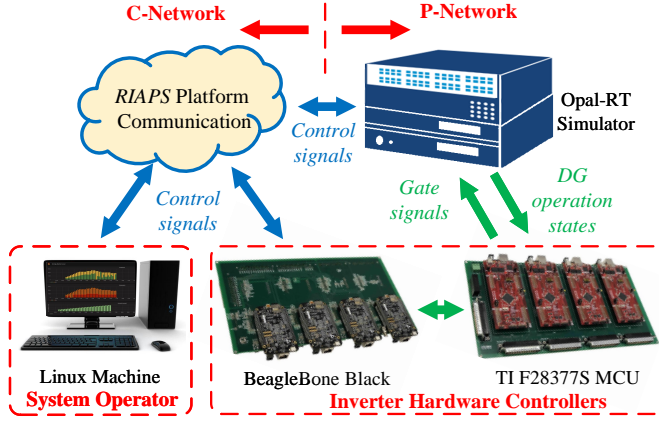


Fig. 7: HIL real-time CPS testbed setup

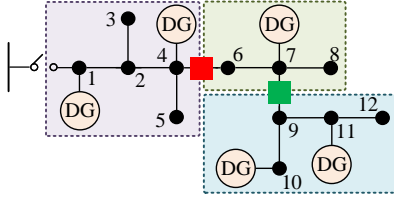


Fig. 8: Physical structure of a 12-bus CPS with 7 agents

$\mathbf{M}^{-1}$  is a diagonal positive-definite scalar. Referring to **Lemma 3**,  $\mathbf{H}_C$  is positive-definite. Similar to the previous case, the system is exponentially stable if  $M_i \approx M_j$ .

System small signal stability with the proposed voltage/reactive power regulations is then derived. The linearized system modeling are presented in matrix form as:

$$\dot{\mathbf{X}}_E = \mathbf{W}_E \mathbf{X}_E \quad (10)$$

where  $\mathbf{X}_E = (\mathbf{E}, \Delta \mathbf{E}_{DG})$  is system states,  $\mathbf{W}_E$  is the corresponding system matrix.

When no reconfiguration is requested, the system matrix is derived as:  $\mathbf{W}_E = \begin{pmatrix} -\mathbf{I} - \mathbf{nN} & \mathbf{I} \\ -k_E \mathbf{T} - k_Q \mathbf{K}' \mathbf{N} & \mathbf{0} \end{pmatrix}$ , where  $\mathbf{T} = \mathbf{n}^{-1}[\mathbf{1}]_{n,n}$  describes the average DG voltage regulation from (4) and  $\mathbf{K}' = \mathbf{H}' + \mathbf{I}$ . Set  $k_E = 0$  and the characteristic polynomial of  $\mathbf{W}_E$  is expressed as:  $\det(s\mathbf{I} - \mathbf{W}_E) = \det(s\mathbf{I} + \mathbf{I} + \mathbf{nN})\det[s^2\mathbf{I} + s(\mathbf{I} + \mathbf{nN}) + k_Q \mathbf{K}' \mathbf{N}] = 0$ . Term  $\det(s\mathbf{I} + \mathbf{I} + \mathbf{nN}) = 0$  satisfied  $\text{Re}(s) < 0$  for all its roots. Referring to **Lemma 1**, matrix  $\mathbf{I} + \mathbf{nN}$  is positive-definite. When  $N_i \approx N_j$ , matrix  $\mathbf{K}' \mathbf{N}$  is positive-definite. Then referring to **Lemma 2**, it is concluded that when  $k_E = 0$  and  $N_i \approx N_j$ , all the roots of the characteristic polynomial satisfy  $\text{Re}(s) < 0$ . Since eigenvalues are continuous function of matrix parameters, the previous conclusion still holds if  $k_E > 0$  is sufficiently small and the system is exponentially stable.

When the target SSW is requested to open, the system matrix becomes:  $\mathbf{W}_E = \begin{pmatrix} -\mathbf{I} - \mathbf{nN} & \mathbf{I} \\ -k_E \mathbf{T} - k_Q \mathbf{K}_O \mathbf{N} & \mathbf{0} \end{pmatrix}$  where  $\mathbf{K}_O = \mathbf{H}' + \frac{k_{\Delta Q}}{k_Q} \mathbf{J}'_O$ . Similar to the frequency/active power regulation case, matrix  $\mathbf{J}'_O$  describes target SSW through power from (6) and is derived that  $\mathbf{J}'_O = 2\text{diag}([\mathbf{1}]_{N_L, N_L}, [\mathbf{1}]_{N_R, N_R})$ . Referring to **Lemma 3**,  $\mathbf{J}'_O$  is positive-definite. Matrix  $\mathbf{K}_O$  and thus  $\mathbf{K}_O \mathbf{N}$  is positive-definite referring to **Lemma 3**. Similar to the previous case, the system is exponentially stable if  $k_E > 0$  is sufficiently small and  $N_i \approx N_j$ .

TABLE I: DG inverter control parameters

Parameters		Values
Droop control	$P$ -f droop gain ( $m$ )	$6.28 \times 10^{-5}$
	$Q$ -V droop gain ( $n$ )	$10 \times 10^{-5}$
	Rated RMS voltage ( $E^*$ )	480 V
	Rated frequency ( $\omega^*$ )	377 rad/s
Inner loop	Voltage loop PI gains ( $k_{P,V}, k_{I,V}$ )	0.14, 120
	Current loop PI gains ( $k_{P,I}, k_{I,I}$ )	2.5, 400
LCL filter	Inverter side inductor ( $L_1$ )	750 $\mu\text{H}$
	Capacitor ( $C$ )	100 $\mu\text{F}$
	Grid side inductor ( $L_2$ )	500 $\mu\text{H}$
Virtual impedance	Virtual inductor ( $R_V, L_V$ )	1 mH
Power circuit	Switching frequency ( $f_{SW}$ )	5000 Hz
	DC link voltage ( $V_{DC}$ )	1200 V
	Rated power output ( $S^*$ )	300 kVA

TABLE II: Selected control gains

$k_f=0.1$	$k_P=0.015$	$k_{\Delta P}=0.002$	$k_{\Delta \theta}=0.025$	$k_V=0.5$
$k_E=0.5$	$k_Q=0.05$	$k_{\Delta Q}=0.4$	$k_{\Delta V}=0.5$	$k_\gamma=50$

When the target SSW is requested to close, the system matrix becomes:  $\mathbf{W}_E = \begin{pmatrix} -\mathbf{I} - \mathbf{nN} & \mathbf{I} \\ -k_Q \mathbf{K}_C \mathbf{N} & \mathbf{0} \end{pmatrix}$  where  $\mathbf{K}_C = \mathbf{H}' + \frac{k_{\Delta V}}{k_Q} \mathbf{J}'_C \mathbf{N}^{-1}$ . Matrix  $\mathbf{J}'_C$  is a matrix that describes the voltage regulation mismatch at target SSW from (3). It is noteworthy that in this case term  $k_E \mathbf{T}$  is not effective as average DG voltage regulation is disabled. As discussed, the voltage at target SSW can be expressed using Millman's theorem and it is derived that  $\mathbf{J}'_C = [\mathbf{1}]_{n,n} \mathbf{C}$  with  $\mathbf{C} = \text{diag}(c_i)$ . When  $N_i \approx N_j$ ,  $\mathbf{N}^{-1}$  is a diagonal positive-definite scalar. Referring to **Lemma 3**,  $\mathbf{J}_C$  is positive-definite. Similar to the previous case, the system is exponentially stable if  $N_i \approx N_j$ . The value of  $k_E$  does not affect the system stability in this scenario.

## V. CASE STUDY

### A. HIL real-time CPS testbed setup

The proposed control strategy is implemented using a HIL real-time CPS testbed, as shown in Fig 7. The testbed consists of two major parts:

- 1) Each inverter-interfaced DG is modeled using inverter switching model and simulated in an FPGA-based simulator with 500 ns simulation time step. SSWs and other non-switching components are simulated in a CPU-based simulator, with 70  $\mu\text{s}$  simulation time step.
- 2) The inverter-interfaced DG primary control is implemented on Texas Instruments (TI) F28377S microcontroller (MCU) unit and generates gate signals for the simulated inverter switching model. Each MCU is associated with one BeagleBone Black (BBB) board that acts as the distributed secondary controller. The BBB boards communicate through a practical cyber network.

The developed controller designs for inverter-interfaced DG agents are implemented on the inverter hardware controllers, while the ones designed for SSW agents are simulated in the simulator. A Linux machine operates as the system operator that initiates the C/P-network reconfiguration request among the corresponding distributed controllers. The C-network implementation and topology variation are achieved using an open-source platform called RIAPS platform [29]. More information on the C/P-networks implementation and execution in the adopted HIL testbed can be found in [30].



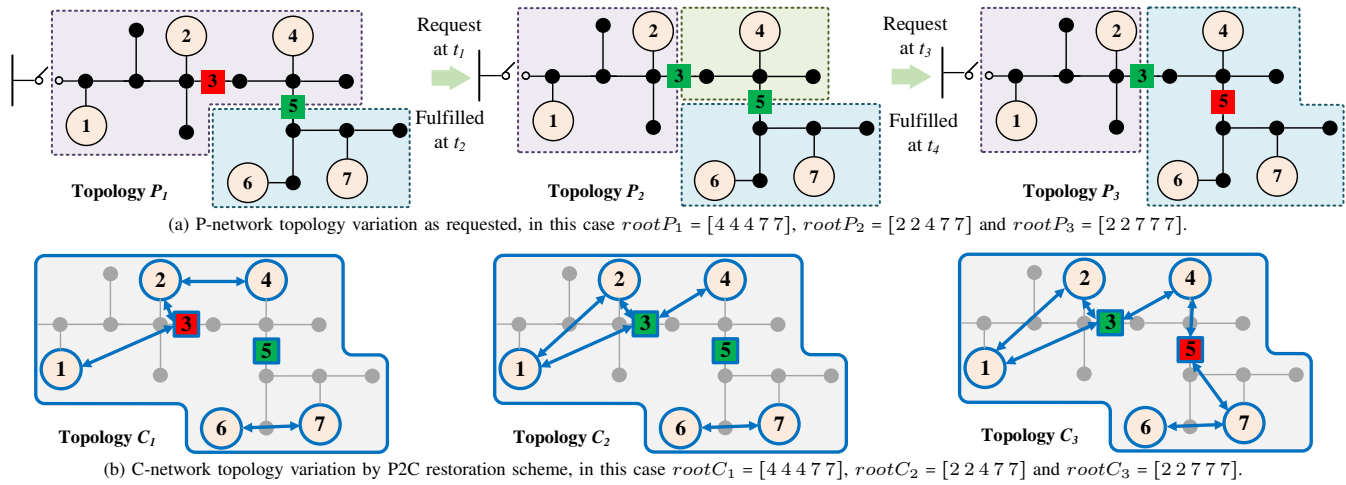


Fig. 9: CPS network variation following requested P-network reconfiguration and corresponding P2C restoration scheme

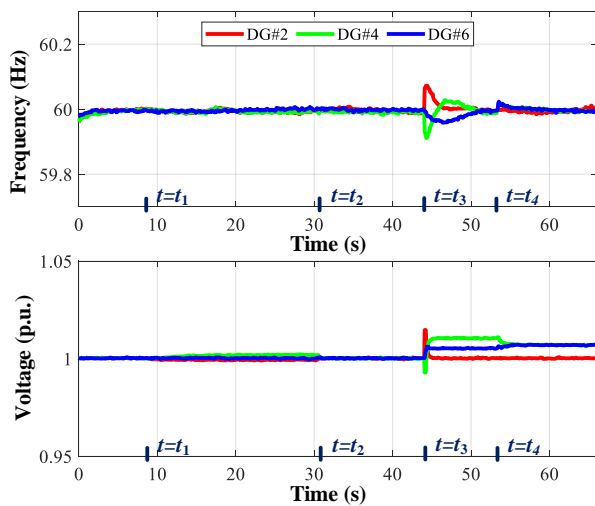


Fig. 10: Recorded DG operating frequency and voltage during P2C variation

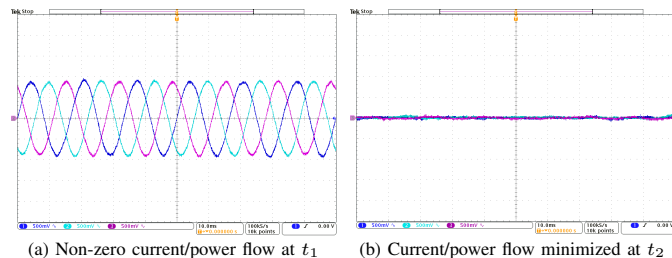


Fig. 11: Real-time three-phase current at SSW agent 3 during P2C variation

The effectiveness of the proposed evaluation framework along with the developed distributed controllers are validated using a 12-bus CPS with 7 agents, as shown in Fig. 8. The test system is divided into three min-MGs by 2 SSWs (agent 3 and 5) and contains 5 inverter-interfaced DGs (agent 1, 2, 4, 6 and 7) with identical power rating. Critical loads are defined at bus 3, 5, 8, 10 and 12 ( $S_{L3} = 2S_{L5} = S_{L8} = S_{L10} = 2S_{L12} = 80 + j40$  kVA). In this work,  $P$ - $f$  and  $Q$ - $V$  droop is adopted in the droop control. Virtual impedance loop is implemented on each DG to ensure droop-based VCM-VSI operation stability [31]. Detailed DG inverter control parameters are presented in Table I. At the initial stage, the system operates in the context of dynamic MGs operation under islanded mode. The selected control gains can be found in Table II.

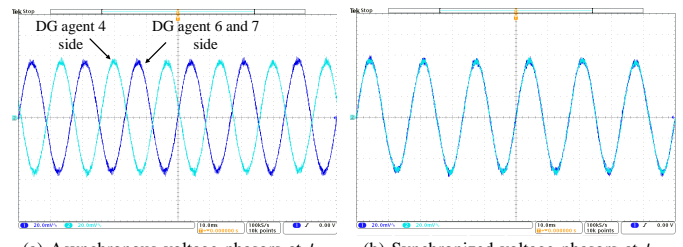


Fig. 12: Real-time phase A voltage across SSW agent 5 during P2C variation

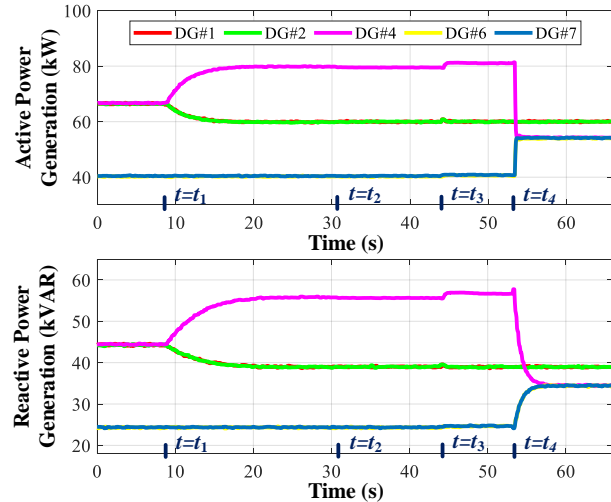


Fig. 13: Recorded DG power outputs during P2C variation

## B. Network reconfiguration using P2C variation

In this case, the system P-network is requested to reconfigure from Topology #1 to #2 at  $t = t_1$  and then to #3 at  $t = t_3$ , as shown in Fig. 9. To ensure system operational feasibility during the P-network reconfiguration, the C-network would be varied accordingly using the proposed C2P variation scheme.

Before the SSW agent 3 receives the reconfiguration request as the target SSW, it is calculated that the DG agent root arrays for C-network under Topology  $C_1$  is  $rootC_1 = [4\ 4\ 4\ 7\ 7]$  while the one for P-network under Topology  $P_2$  is  $rootP_2 = [2\ 2\ 4\ 7\ 7]$ . It is determined using the proposed P2C variation scheme that the target P-network under  $P_2$  can not be properly operated with the operating C-network under  $C_1$ , and the C-network should first be updated to  $C_2$ . Once the C-network variation is done, the reconfiguration

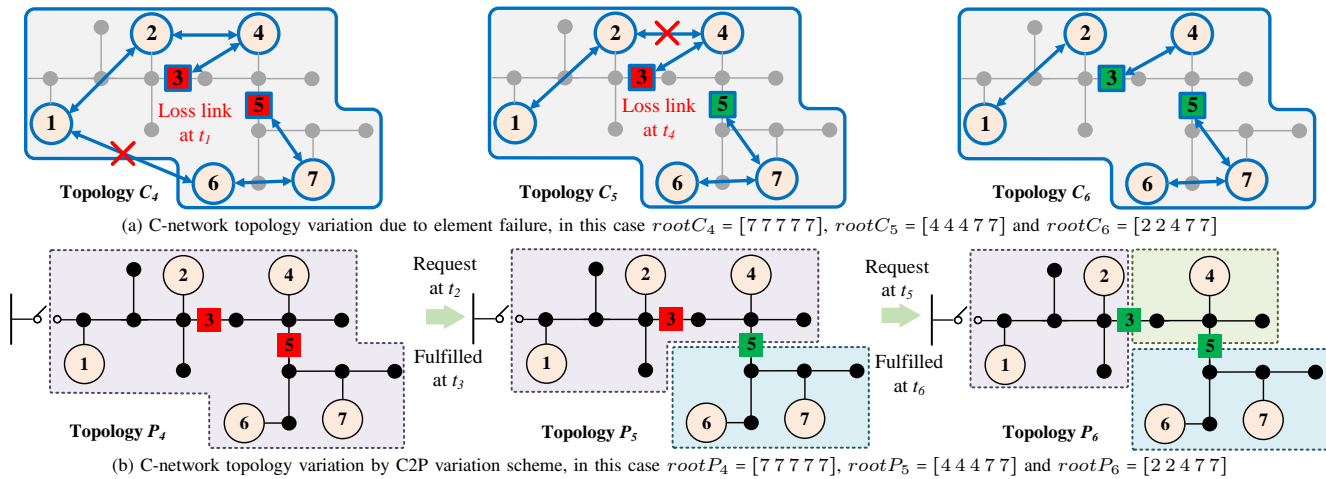


Fig. 14: CPS network variation following unplanned C-network reconfiguration and C2P variation scheme

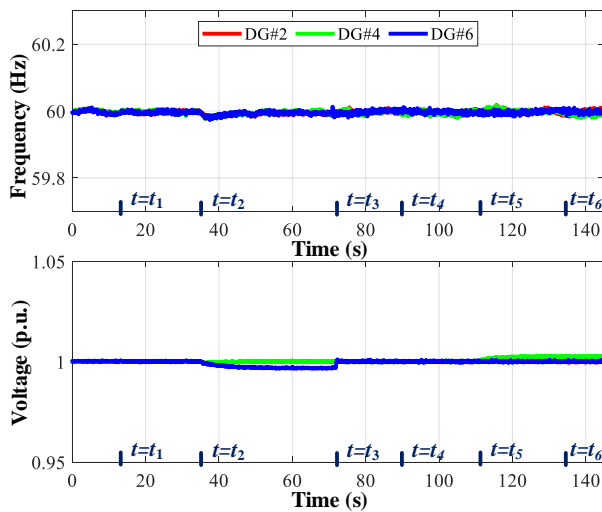


Fig. 15: Recorded DG operation frequency and voltage during C2P variation

request is sent to SSW agent 3 at  $t_1$  and fulfilled at  $t_2$  as the closed SSW re-opens. Similarly, applying the proposed P2C variation scheme before the P-network varies from  $P_2$  to  $P_3$ , it is found that  $rootC_2 = [2 \ 2 \ 4 \ 7 \ 7]$  while  $rootP_3 = [2 \ 2 \ 7 \ 7 \ 7]$ . Thus the C-network varies to  $C_3$  before the reconfiguration on SSW agent 5 is requested at  $t_3$  and fulfilled at  $t_4$ .

The system operating frequency and voltage measured at DG agent 2, 4 and 6 are presented in Fig. 10 representing system operating states within each min-MG. It is observed that the system operating frequency and voltage within each min-MGs have been maintained closely around rated. The frequency and voltage variations observed at  $t_3$  are expected, as they are introduced due to the designed phase and voltage magnitude regulation for SSW agent 5 seamless re-close. Real-time three-phase current waveform across SSW agent 1 at  $t_1$  and  $t_2$  are presented in Fig. 11. It is observed that the non-zero current/power flow at SSW agent 1 has been minimized before it changes status and seamless SSW agent 1 re-open is achieved. Real-time phase A voltage waveform across SSW agent 2 at  $t_3$  and  $t_4$  are presented in Fig. 12. It is observed that at SSW agent 2, the asynchronous voltage phasors are re-synchronized before the SSW changes status and seamless SSW agent 2 re-close is achieved.

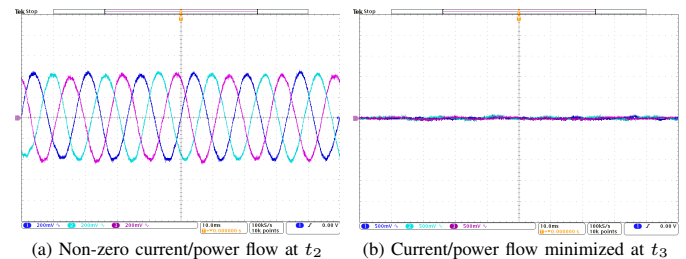


Fig. 16: Real-time three-phase current at SSW agent 5 during C2P variation

At last, the recorded DG power outputs during the P2C variation are shown in Fig. 13. It is observed that proportional active/reactive power sharing among physically connected DGs are constantly guaranteed with respect to P-network variation. Initially the system operates under Topology #1, DG agent 1, 2 and 4 are connected while DG agent 6 and 7 are connected. After SSW agent 3 opens at  $t_2$  and the system operates under Topology #2, DG agent 1 and 2 are connected, DG agent 6 and 7 are connected, and DG agent 4 operates stand-alone. After SSW agent 5 closes at  $t_4$  and the system operates under Topology #3, DG agent 1 and 2 are connected, while DG agent 4 is reconnected to DG agent 6 and 7.

### C. Network reconfiguration using C2P variation

In this case, the system C-network varies due to element failure, as shown in Fig. 14 and feasibility criterion can not be met. The system P-network shall actively reconfigure using the proposed C2P restoration scheme. Initially the system operates with  $rootC_4 = [7 \ 7 \ 7 \ 7 \ 7] = rootP_4$ . At  $t_1$ , the communication link between DG agent 1 and 6 is disabled. The C-network varies from  $C_4$  to  $C_5$  and root array becomes  $rootC_5 = [4 \ 4 \ 4 \ 7 \ 7]$ . It is determined using the proposed C2P variation scheme that the operating C-network under  $C_5$  can not be properly operated with the operating P-network under  $P_4$ , and the P-network should be actively reconfigured to  $P_5$ . The reconfiguration request is sent to SSW agent 5 at  $t_2$  and fulfilled at  $t_3$  as the target SSW opens. At  $t_4$ , the communication link between DG agent 2 and 4 is disabled and the C-network varies from  $C_5$  to  $C_6$ . It is determined that to restore the system back to feasible operation, the P-network needs to reconfigure from  $P_5$  to  $P_6$ . The reconfiguration request is sent at  $t_5$  and fulfilled at  $t_6$ .

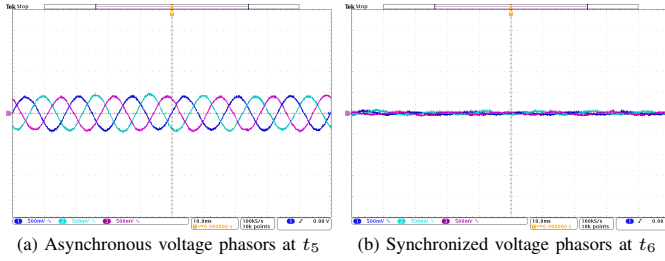


Fig. 17: Real-time three-phase current at SSW agent 3 during C2P variation

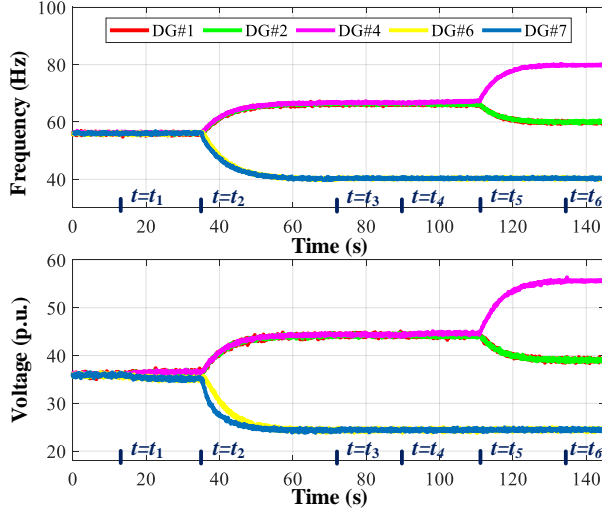


Fig. 18: Recorded DG power outputs during C2P variation

The system operating frequency and voltage measured at DG agent 2, 4 and 6 are presented in Fig. 15. It is observed that the system operating frequency and voltage within each min-MGs have been maintained closely around rated, even after the unplanned communication lost at  $t_1$  and  $t_4$ . Real-time three-phase current waveform across SSW agent 5 at  $t_2$  and  $t_3$  and SSW agent 3 at  $t_5$  and  $t_6$  are presented in Fig. 16 and Fig. 17, respectively. It is observed that the non-zero current/power flow at the SSW agents have been minimized before they change status and seamless SSW agents re-open are achieved, respectively.

At last, the recorded DG power outputs during the C2P variation are shown in Fig. 18. It is observed that proportional active/reactive power sharing among physically connected DGs are constantly guaranteed with respect to P-network variation. Initially the system operates under Topology #4, all the DG are connected and share power equally. After the unplanned communication lost between DG agent 1 and 6 at  $t_1$ , DG agent 1, 2 and 4 are cyber connected while DG agent 6 and 7 are cyber connected, which leads to undesired power sharing among DGs. After SSW agent 5 opens at  $t_3$  and the system operates under Topology #5, proportional power sharing among physically connected DGs are achieved where two subgroups are formed: DG agent 1, 2 and 4 and DG agent 6 and 7. Similarly, undesired power sharing among DG agent 1, 2 and 4 is observed after the unplanned communication lost between DG agent 2 and 4 at  $t_4$ . After SSW agent 3 opens at  $t_6$  and the system operates under Topology #6, proportional power sharing among physically connected DGs are achieved where three subgroups are formed: DG agent 1 and 2, DG agent 4 (stand-alone) and DG agent 6 and 7.

## VI. CONCLUSION

In this paper, the CPS operation with reconfigurable C/P-networks is discussed. The system is assumed to be controlled under distributed consensus-based algorithms and its P-network reconfiguration is implemented in the context of dynamic MGs operation. A network matrix is defined to describe the C/P-network topologies and a disjoint-set data structure is defined to track the connectivity among agents. An evaluation framework is proposed. An operational feasibility criterion is derived for the system with static C/P-networks. Two types of variation schemes (C2P and P2C) that ensure system operational feasibility during both C- and P-network reconfigurations are developed. Detailed distributed controller designs are developed for SSW agents and DG agents, respectively. The developed control algorithms are able to realize the network seamless reconfiguration as per the system operator's requests and provide secondary regulation with respect to system real-time topology. At last, the proposed evaluation framework along with the developed distributed controller is validated using a 12-bus CPS on a HIL real-time testbed.

## APPENDIX A PROOF OF THEOREM 1

As reviewed, following lemma regarding CPS operation under consensus-based control is concluded:

**Lemma 1** Proper operation of CPS with all the DG agents being connected in P-network requires their C-network to also remain connected, and vice versa.

As previously mentioned, **Lemma 1** is only derived for CPS with constant P-network where all the DG agents remain physically connected. For CPS operation with reconfigurable C/P-networks, once the reconfigurations are done and the CPS operates with certain C/P-network topologies, the P-network could be divided into isolated subgraphs. Each subgraph contains connected DG agents. Apply **Lemma 1** to each subgraph in the P-network and the proof is completed. SSW agents are not directly affecting CPS operational feasibility when no P-network reconfiguration is requested, however, the status of each SSW agent is still critical as they determine the physical connectivity among DG agents.

## APPENDIX B PSEUDO CODE OF DEVELOPED ALGORITHMS

Construction rules to generate the DG agent exclusive root array from a network matrix are presented as follows using pseudo code:

### Algorithm 1 Generate parent array for DG agents

```

par(1:n) = 1:n, id(1:n) = 1:n // Initialization
for each agent i in par() and i < j ≤ n
    while N(i,i) = 1 ∩ N(i,j) = 1 ∩ N(j,j) = 1
        if par(i) ≤ j
            k = i
            while par(par(k)) ≠ par(k)
                k = par(k)
            end while

```

```

        par(par(k)) = j
    else
        par(j) = par(i)
    end while
end for
switch each agent i in par() // Remove SSW agents
case agent i is DG agent  $\cap$  par(i) is SSW agent
    set par(i) as the DG agent connected to agent i
    with the largest ID number
case par(i) is SSW agent
    remove par(i), remove id(i)
end switch
root=par
for each agent i in root()
    while root(root(i))  $\neq$  root(i)
        root(i) = root(root(i))
    end while
end for
return root

```

The root array is constructed so that:

- It contains only DG agents while SSW agents are eliminated without violating the DG agents connectivity;
- Agent with the largest ID number in a connected sub-graph is assigned as the root agent.

Construction rules to generate the desired C-network for P2C variation are presented as follows using pseudo code:

---

**Algorithm 2** P2C variation for C-network reconfiguration

---

```

N'_C = N_C // Initialization
while rootC  $\neq$  rootP // Check operational feasibility
    find the largest i s.t. rootC(i)  $\neq$  rootP(i)
    if id(i)  $\neq$  rootC(i)
        find paths pathC[] s.t. agent id(i) and agent
        rootC(i) are connected in N'_C
        disconnect all the edges in pathC[], update N'_C
    end if
    if id(i)  $\neq$  rootP(i)
        direct connect agent id(i) and agent rootP in N'_C
    end if
    generate rootC() for N'_C
end while
for agent i = 1 : n //Enable SSW connectivity
    if N'_P(i, s) = 1  $\cap$  agent i is not SSW agent
        N'_C(i, s) = N'_C(s, i) = 1
    end if
end for
return N'_C

```

Different algorithms can be applied to find  $pathC[]$  (e.g., depth-first search, breadth-first search, etc.). By **Algorithm 2**, all the DGs agents that belong to the same min-MGs with the target SSW will be cyber connected in  $N'_C$ , such approach will not, in turn, break the reliable operation criterion as the operation status of SSW agent is defined to be consistent on both C-network and P-network.

Construction rules to generate the desired P-network reconfiguration in terms of target SSWs selection for C2P variation

are presented as follows using pseudo code:

---

**Algorithm 3** Selection of target SSWs for C2P variation

---

```

N'_P = N_P, SSW = [] // Initialization
for agent i = 1 : n as SSW agent
    for agent j = 1 : n as DG agent
        if N'_C(i, j) = 1  $\cap$  root(i) = root(j) in N_P
            store i into SSW()
        end if
    end for
end for
if SSW() is null
    break // No feasible restoration
else Generate all possible combinations of indices,  $\eta$  in
SSW() and stored in data[]
end if
for each  $\eta$  and its corresponding N'_P
    if rootP' = rootC'
        keep  $\eta$  in data[]
    else
        remove  $\eta$  in data[]
    end if
end for
return data[]

```

The generated  $data[]$  contains all the possible combinations of controllable SSWs that result in a proper P-network reconfiguration. After the target SSWs have been selected, the system operator shall implement the one that requires the least number of SSW operation for restoration.

## REFERENCES

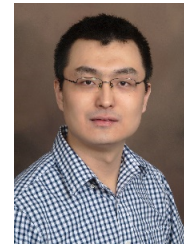
- [1] X. Yu and Y. Xue, "Smart grids: A cyber-physical systems perspective," *Proceedings of the IEEE*, vol. 104, no. 5, pp. 1058–1070, May 2016.
- [2] Z. Cheng, J. Duan, and M. Chow, "To centralize or to distribute: That is the question: A comparison of advanced microgrid management systems," *IEEE Industrial Electronics Magazine*, vol. 12, no. 1, pp. 6–24, March 2018.
- [3] D. T. Ton and M. A. Smith, "The US department of energy's microgrid initiative," *The Electricity Journal*, vol. 25, no. 8, pp. 84–94, 2012.
- [4] M. E. Nassar and M. M. A. Salama, "Adaptive self-adequate microgrids using dynamic boundaries," *IEEE Transactions on Smart Grid*, vol. 7, no. 1, pp. 105–113, Jan 2016.
- [5] Y. Ma, X. Hu, H. Yin, L. Zhu, Y. Su, F. Wang, L. M. Tolbert, and Y. Liu, "Real-time control and operation for a flexible microgrid with dynamic boundary," in *2018 IEEE Energy Conversion Congress and Exposition (ECCE)*, Sep. 2018, pp. 5158–5163.
- [6] Y. Du, X. Lu, J. Wang, and S. Lukic, "Distributed secondary control strategy for microgrid operation with dynamic boundaries," *IEEE Transactions on Smart Grid*, vol. 10, no. 5, pp. 5269–5282, Sep. 2019.
- [7] Y. Kim, J. Wang, and X. Lu, "A framework for load service restoration using dynamic change in boundaries of advanced microgrids with synchronous-machine DGs," *IEEE Transactions on Smart Grid*, vol. 9, no. 4, pp. 3676–3690, July 2018.
- [8] J. W. Simpson-Porco, Q. Shafiee, F. Dörfler, J. C. Vasquez, J. M. Guerrero, and F. Bullo, "Secondary frequency and voltage control of islanded microgrids via distributed averaging," *IEEE Transactions on Industrial Electronics*, vol. 62, no. 11, pp. 7025–7038, Nov 2015.
- [9] Y. Du, X. Lu, H. Tu, J. Wang, and S. Lukic, "Dynamic microgrids with self-organized grid-forming inverters in unbalanced distribution feeders," *IEEE Journal of Emerging and Selected Topics in Power Electronics*, pp. 1–1, 2019.
- [10] G. Lou, W. Gu, Y. Xu, M. Cheng, and W. Liu, "Distributed mpc-based secondary voltage control scheme for autonomous droop-controlled microgrids," *IEEE Transactions on Sustainable Energy*, vol. 8, no. 2, pp. 792–804, April 2017.



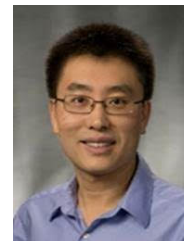
- [11] R. Olfati-Saber, J. A. Fax, and R. M. Murray, "Consensus and cooperation in networked multi-agent systems," *Proceedings of the IEEE*, vol. 95, no. 1, pp. 215–233, Jan 2007.
- [12] R. O. Saber and R. M. Murray, "Consensus protocols for networks of dynamic agents," 2003.
- [13] M. Lu and L. Liu, "Distributed feedforward approach to cooperative output regulation subject to communication delays and switching networks," *IEEE Transactions on Automatic Control*, vol. 62, no. 4, pp. 1999–2005, April 2017.
- [14] H. Cai and G. Hu, "Distributed nonlinear hierarchical control of ac microgrid via unreliable communication," *IEEE Transactions on Smart Grid*, vol. 9, no. 4, pp. 2429–2441, July 2018.
- [15] S. Marzal, R. Salas, R. González-Medina, G. Garcerá, and E. Figueres, "Current challenges and future trends in the field of communication architectures for microgrids," *Renewable and Sustainable Energy Reviews*, vol. 82, pp. 3610–3622, 2018.
- [16] C. Chen, J. Wang, and D. Ton, "Modernizing distribution system restoration to achieve grid resiliency against extreme weather events: An integrated solution," *Proceedings of the IEEE*, vol. 105, no. 7, pp. 1267–1288, 2017.
- [17] Y. Xu, C. C. Liu, K. P. Schneider, F. K. Tuffner, and D. T. Ton, "Microgrids for service restoration to critical load in a resilient distribution system," *IEEE Transactions on Smart Grid*, vol. 9, no. 1, pp. 426–437, Jan 2018.
- [18] C. Wang, T. Zhang, F. Luo, F. Li, and Y. Liu, "Impacts of cyber system on microgrid operational reliability," *IEEE Transactions on Smart Grid*, vol. 10, no. 1, pp. 105–115, Jan 2019.
- [19] B. Falahati and Yong Fu, "A study on interdependencies of cyber-power networks in smart grid applications," in *2012 IEEE PES Innovative Smart Grid Technologies (ISGT)*, Jan 2012, pp. 1–8.
- [20] J. Guo, W. Liu, F. R. Syed, and J. Zhang, "Reliability assessment of a cyber physical microgrid system in island mode," *CSEE Journal of Power and Energy Systems*, vol. 5, no. 1, pp. 46–55, March 2019.
- [21] Z. Galil and G. F. Italiano, "Data structures and algorithms for disjoint set union problems," *ACM Computing Surveys (CSUR)*, vol. 23, no. 3, pp. 319–344, 1991.
- [22] J. Sun, "Impedance-based stability criterion for grid-connected inverters," *IEEE Transactions on Power Electronics*, vol. 26, no. 11, pp. 3075–3078, Nov 2011.
- [23] Z. Li, C. Zang, P. Zeng, H. Yu, and H. Li, "MAS based distributed automatic generation control for cyber-physical microgrid system," *IEEE/CAA Journal of Automatica Sinica*, vol. 3, no. 1, pp. 78–89, January 2016.
- [24] J. M. Guerrero, J. C. Vasquez, J. Matas, L. G. De Vicuña, and M. Castilla, "Hierarchical control of droop-controlled AC and DC microgrids—a general approach toward standardization," *IEEE Transactions on industrial electronics*, vol. 58, no. 1, pp. 158–172, 2011.
- [25] B. Liu, W. Lu, and T. Chen, "Pinning consensus in networks of multiagents via a single impulsive controller," *IEEE Transactions on Neural Networks and Learning Systems*, vol. 24, no. 7, pp. 1141–1149, July 2013.
- [26] R. A. Horn, R. A. Horn, and C. R. Johnson, *Matrix analysis*. Cambridge university press, 1990.
- [27] J. W. Simpson-Porco, Q. Shafiee, F. Dörfler, J. C. Vasquez, J. M. Guerrero, and F. Bullo, "Secondary frequency and voltage control of islanded microgrids via distributed averaging," *IEEE Transactions on Industrial Electronics*, vol. 62, no. 11, pp. 7025–7038, 2015.
- [28] J. Millman, "A useful network theorem," *Proceedings of the IRE*, vol. 28, no. 9, pp. 413–417, 1940.
- [29] H. Tu, Y. Du, H. Yu, A. Dubey, S. Lukic, and G. Karsai, "Resilient information architecture platform for the smart grid (riaps): A novel open-source platform for microgrid control," *IEEE Transactions on Industrial Electronics*, pp. 1–1, 2019.
- [30] Y. Du, H. Tu, S. Lukic, D. Lubkeman, A. Dubey, and G. Karsai, "Development of a controller hardware-in-the-loop platform for microgrid distributed control applications," in *2018 IEEE Electronic Power Grid (eGrid)*, Nov 2018, pp. 1–6.
- [31] J. He and Y. W. Li, "Analysis, design, and implementation of virtual impedance for power electronics interfaced distributed generation," *IEEE Transactions on Industry Applications*, vol. 47, no. 6, pp. 2525–2538, 2011.



**Yuhua Du** (S'17) received the B.S degree in electrical engineering from Xi'an Jiaotong University, China in 2013 and Ph.D. degree in electrical and computer engineering from North Carolina State University, USA in 2019. He was a Research Aide with Argonne National Laboratory in 2018. He is currently a Postdoctoral Fellowship in Temple University. His research interests include voltage source converter modeling and control, microgrid distributed secondary control and development of microgrid hardware-in-the-loop testbed.



**Xiaonan Lu** (S'12-M'13) received his B.E. and Ph.D. degrees in electrical engineering from Tsinghua University, Beijing, China, in 2008 and 2013, respectively. From September 2010 to August 2011, he was a guest Ph.D. student at the Department of Energy Technology, Aalborg University, Denmark. From October 2013 to December 2014, he was a Postdoc Research Associate at the Department of Electrical Engineering and Computer Science, University of Tennessee, Knoxville. From January 2015 to July 2018, he was with Argonne National Laboratory, first as a Postdoc Appointee and then as an Energy Systems Scientist. In July 2018, he joined the College of Engineering in Temple University as an Assistant Professor. Dr. Lu is the Associate Editor of IEEE Transactions on Industrial Electronics, the Associate Editor of IEEE Transactions on Industry Applications and the Editor of IEEE Transactions on Smart Grid. He is currently serving as the Vice Chair of Industrial Power Converters Committee (IPCC) in IEEE Industry Applications Society (IAS).



**Jianhui Wang** Jianhui Wang (M'07-SM'12) received the Ph.D. degree in electrical engineering from Illinois Institute of Technology, Chicago, Illinois, USA, in 2007.

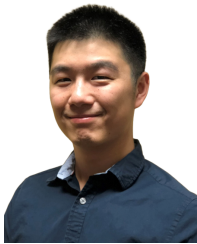
Presently, he is an Associate Professor with the Department of Electrical and Computer Engineering at Southern Methodist University, Dallas, Texas, USA. Prior to joining SMU, Dr. Wang had an eleven-year stint at Argonne National Laboratory with the last appointment as Section Lead – Advanced Grid Modeling. Dr. Wang is the secretary of the IEEE Power & Energy Society (PES) Power System Operations, Planning Economics Committee. He has held visiting positions in Europe, Australia and Hong Kong including a VELUX Visiting Professorship at the Technical University of Denmark (DTU). Dr. Wang is the Editor-in-Chief of the IEEE Transactions on Smart Grid and an IEEE PES Distinguished Lecturer. He is also a Clarivate Analytics highly cited researcher for 2018.



**Bo Chen** (M'17) received the Ph.D. degree in electrical engineering from Texas AM University, College Station, USA, in 2017. He received the B.S. and M.S. degrees from North China Electric Power University, Baoding, China. In 2017, he worked as a postdoc researcher at the Argonne National Laboratory, IL, USA. Currently, he is an Energy Systems Scientist at the Energy Systems Division, Argonne National Laboratory, IL, USA. His research interests include modeling, control, and optimization of power systems, cybersecurity, and cyber-physical

systems.





**Hao Tu** (S'17) received his bachelor, master and Ph.D. degree from Xi'an Jiaotong University, China in 2012, RWTH Aachen University, Germany in 2015, and North Carolina State University in 2020, respectively, all in electrical engineering.

His research interests include control of power electronics converters, energy storage systems, and microgrids.



**Srdjan Lukic** (M'07, SM'19) received the Ph.D. degree in electrical engineering from the Illinois Institute of Technology, Chicago, IL, USA, in 2008, and is currently a Professor with the Department of Electrical and Computer Engineering, North Carolina State University, Raleigh, NC, USA. He serves as the Deputy Director of the National Science Foundation Future Renewable Electric Energy Delivery and Management (FREEDM) Systems Engineering Research Center, headquartered at North Carolina State University.

His current research interests include design, and control of power electronic converters and electromagnetic energy conversion with application to microgrids, wireless power transfer, energy storage systems, and electric automotive systems. He was a Distinguished Lecturer with the IEEE Vehicular Technology Society from 2011 to 2015.